Investigation of the Prebreakdown Gap Currents between Clean and Cesium-Coated Tungsten Electrodes

CAROL J. BENNETTE,* R. W. STRAYER,† E. C. COOPER,* AND L. W. SWANSON‡
Field Emission Corporation, McMinnville, Ore.

Prebreakdown currents have been measured between tungsten electrodes with varying amounts of adsorbed cesium and oxygen under both high vacuum conditions and in the presence of a cesium pressure of 2×10^{-6} torr. Under the conditions investigated, the prebreakdown currents were due to field emission from small protrusions on the cathode; the corresponding current-voltage characteristics were stable and reproducible. The main effect of surface adsorbates was to change the work function of the emitting surface. The gap voltage for a permitted gap current was thus found to be a function of surface roughness and of amount of contamination upon the electrodes and to be directly proportional to gap spacing. Typical values of the gross field for 0.1μa gap current between thermally smoothed surfaces are 3.1 Mv/cm for clean tungsten and 0.62 Mv/cm for an optimum cesium coverage. The local electric fields at the tips of protrusions on the electrodes, as determined by analysis of the resulting current-voltage characteristics, are much higher, up to 70 Mv/cm. Evidence for field and temperature induced geometrical changes of the surface is given and discussed.

Introduction

UNDESIRED leakage currents and electrical breakdown between electrodes in high vacuum is a subject receiving increased interest at the present time, primarily because of the need for operation of high-voltage apparatus in outer space. The systems studied range from clean electrodes in ultrahigh vacuum to electrodes in relatively low vacuum where surface conditions are not well defined. This paper attempts to bridge the gap between these extremes by reporting measurements of time stable gap currents, hereafter referred to as prebreakdown gap currents, between atomically clean tungsten electrodes in ultrahigh vacuum and electrodes with known amounts of cesium and/or oxygen. An understanding of the nature of the prebreakdown currents is helpful in understanding the origin of leakage current and processes that lead to the actual high-vacuum arc.

Experimental Procedures

The experimental tube used for the present study is shown in Fig. 1. The tube was a diode consisting of a spherical electrode (diameter equal to 25 mils) and a planar electrode with variable gap spacing. This configuration permitted independent variation of the electric field at the electrode surfaces and of the total gap voltage, so that the effects of these two parameters on prebreakdown gap currents could be determined separately; it also permitted accurate determination of the gross field at both surfaces. The spacing was varied and measured by means of a stainless-steel bellows and a micrometer head.

The tube envelope was constructed from aluminosilicate glass to reduce helium diffusion after tube evacuation and sealoff. During the investigation of effects of higher cesium pressures, a portion of the tube envelope was kept hot by an external heater in order to prevent the development of electrical leakage paths on the inside of the glass walls. Cesium was deposited on both electrodes by heating the cesium reservoir and keeping the electrodes cold, or onto one electrode only by maintaining the other at a sufficiently high temperature to thermally desorb the cesium. For the experiments reported here, both electrodes were always coated with the same degree of coverage of cesium and/or oxygen. The temperature of the spherical electrode was determined by measurement of the resistance of a segment of the supporting tungsten filament. The degree of cesium coverage on the electrodes was determined by measuring the

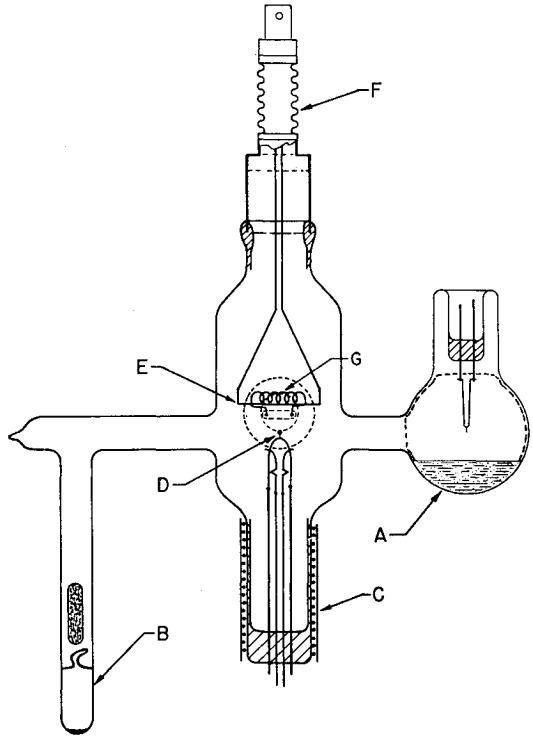

Fig. 1 Voltage breakdown study tube with variable spacing electrodes: *A*, field emission microscope; *B*, cesium ampule; *C*, heatable section of in-seal; *D*, spherical electrode; *E*, plane electrode; *F*, stainless-steel bellows; *G*, 10-mil tungsten filament for electron bombardment heating of plane electrode.

Presented as preprint 64-694 at the AIAA Fourth Electric Propulsion Conference in Philadelphia, Pa., August 31–September 2, 1964; revision received September 8, 1964. This work was supported by NASA Lewis Research Center. The authors wish to express their thanks to F. M. Charbonnier for valuable suggestions in preparing this manuscript.

* Physicist.
† Physicist. Member AIAA.
‡ Physical Chemist. Member AIAA.

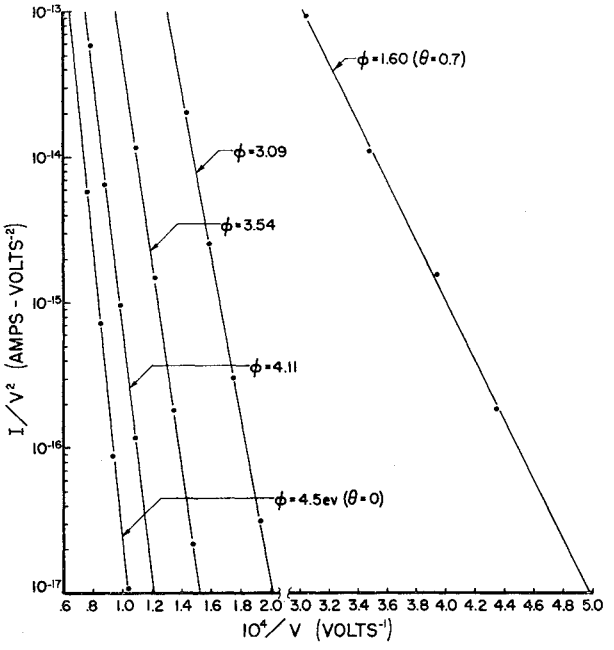

Fig. 2 Fowler-Nordheim plots of *I-V* data obtained with the sphere negative at an electrode spacing of 2.8 mils at the indicated cesium coverages and work functions.

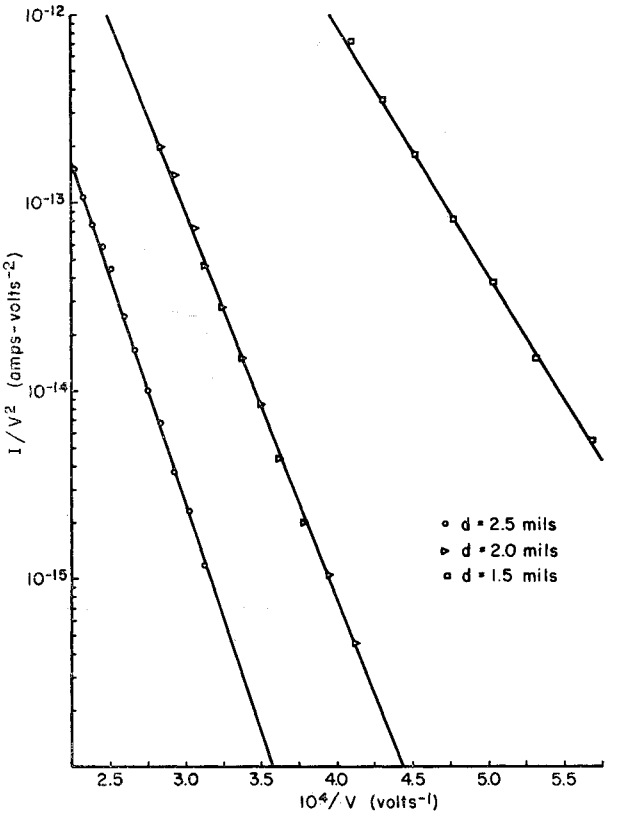

Fig. 3 Room temperature Fowler-Nordheim plots of *I-V* data obtained with the sphere negative at the indicated electrode spacings for an ambient cesium pressure of 2×10^{-6} torr.

work function of the emitting surface and then using the known relationship between work function and coverage for cesium on tungsten.[1] When measurements were performed in an ambient cesium pressure, the latter was varied by controlling the temperature of the cesium reservoir, with the tube itself being operated at a temperature above that of the reservoir. With cesium on the electrodes, measurements were taken while the tube was shielded from light to eliminate excessive photo currents.

The small field emission microscope, containing a tungsten emitter and attached to the main bulb as an appendage, monitored the vacuum conditions and helped determine the degree and type of possible contamination on the electrode surfaces, without itself acting as a source of contamination. Vacuum conditions were better than 10^{-10} torr in all cases reported here, except when a higher pressure of cesium vapor was purposely introduced for some of the measurements.

The prebreakdown current can thus be measured as a function of voltage, electric field, electrode temperature, degree of cesium coverage, and cesium vapor pressure. The procedure generally followed consisted of the measurement of gap current I between electrodes free of contaminants, as a function of gap voltage V for a series of gap spacings d, all other parameters being held constant. Then one of the parameters (such as degree of cesium coverage) was modified and the measurement repeated; thus, the effect of the particular parameter upon the prebreakdown current was determined.

In connection with the present studies, field emission microscopy has been used to establish relationships between coverage and work function for cesium and/or oxygen on tungsten, and to study formation of protrusions on clean tungsten surfaces. Details of construction and uses of field emission microscopes are presented elsewhere.[2-4]

Results and Discussion

Prebreakdown gap currents between clean and cesium-coated tungsten electrodes were measured as functions of the following parameters: electrode gap spacings from 1.5 to 10.0 mils, surface work functions from 1.2 to 5.1 ev (depending upon the amount of cesium and/or oxygen on the surface), ultrahigh vacuum (pressures less than 10^{-10} torr) and ambient cesium pressures up to 2×10^{-6} torr, temperatures of the clean substrate between 293° and 1000°K, both polarities of electric field, and various degrees of surface roughness.

Nature of the Gap Current

For gap currents between 10^{-10} and 10^{-4} amp, the current was found to be due to field emission only under the conditions mentioned previously. This fact was established by analyzing the *I-V* data according to the Fowler-Nordheim equation (A5) (see Appendix) for field emission, whereby the linearity of the plots of log I/V^2 vs $10^4/V$ ("Fowler-Nordheim plots") establishes the field emission nature of the gap current, since no other current-initiating mechanism is known to have this particular functional relationship. The linearity of the present data is illustrated in typical plots in Figs. 2 and 3. Figure 2 summarizes data obtained at a fixed gap spacing (d = 2.8 mils) for work functions between 4.5 and 1.6 ev, corresponding to cesium coverages on the spherical electrode ranging from 0 to 0.7 monolayer; similar data were obtained for other gap spacings, and also for cesium on oxygen-contaminated electrodes for which the work functions varied from 5.1 to 1.2 ev. Figure 3 illustrates the linearity of Fowler-Nordheim plots of the $I(V)$ data obtained for an ambient cesium pressure of 2×10^{-6} torr at various electrode spacings and with the electrodes at room temperature. For clean tungsten surfaces at temperatures between 293° and 1000°K, the *I-V* data obeyed the temperature dependent field emission equation (A1).

For fixed values of gap current, temperature, and surface work function, the gap voltage was a linear function of gap spacing, as shown in Fig. 4 for $I = 1.0$ μa and a cesium coverage of 0.7 monolayer. This direct proportionality between V and d at constant current, showing that the gross field $F_0 = V/d$ to draw a constant gap current I was independent of d over the range of d investigated, is additional evidence

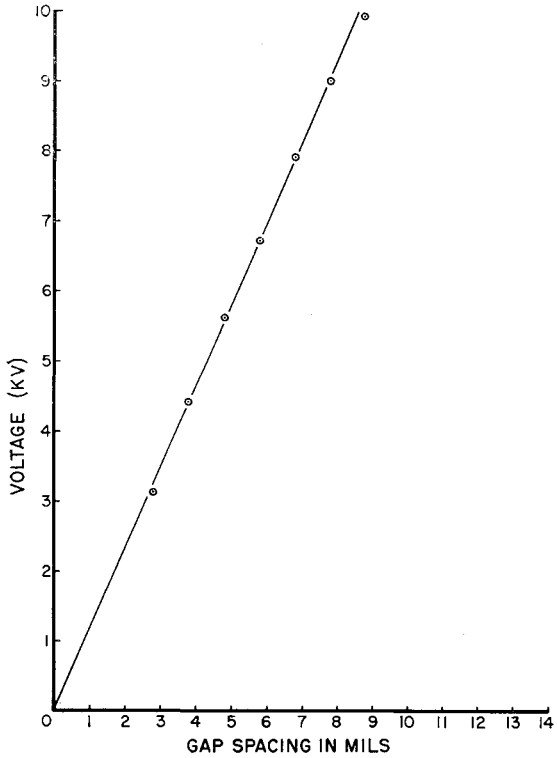

Fig. 4 Room temperature plot of voltage required to maintain 10^{-6} amps vs electrode spacing with the sphere negative and cesium-coated such that its work function is 1.6 ev.

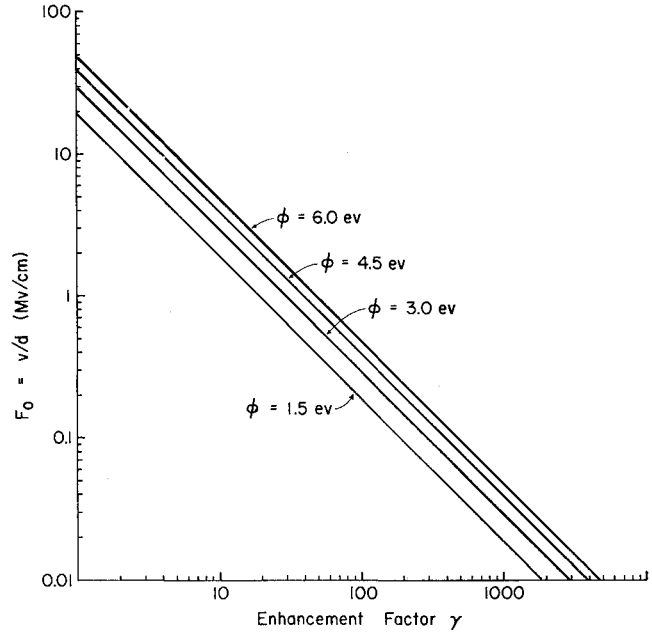

Fig. 5 Gross field, $F_0 = V/d$, as a function of enhancement factor γ for various electrode work functions for 1 μa emission current, assuming an emitting area of 10^{-10} cm^2.

that the gap current was due to field emission and further indicates that I originated at protrusions on the electrode surface which were small compared to the minimum gap spacing investigated. There may be a large number of protrusions on the surface; however, since in field emission the current is a highly nonlinear function of local field and therefore of electrode geometry (see Appendix), emission from a single protrusion, or at most a small group of protrusions of similar geometry, will predominate.

Surface Field Enhancement Factors

The gross field, obtained from the slopes of such curves as in Fig. 4, is considerably less than the actual field F at the emission sites, determined by analyzing the I-V data according to Eqs. (A4–A6).

Protrusions on the electrode surfaces reduce the gap voltage required to sustain a given gap current by enhancing the field locally. The factor by which the field is locally enhanced due to surface roughness is defined as the surface enhancement factor γ and is the ratio of the maximum electric field F at the tip of a protrusion to the gross field $F_0 = V/d$ in the gap, i.e., $\gamma = F/F_0$. Thus, F_0 for a given field-emitted gap current is a function of both the work function of the emitting surface and its enhancement factor, as shown in Fig. 5. Enhancement factors observed in this work, as obtained by Eq. (A7), range from 10 to 340 depending on prior treatment of the electrode surfaces. For a relatively low enhancement factor of 12 on the spherical electrode and a gap current of 0.1 μa, F_0 for clean tungsten was 3.1 Mv/cm, whereas F_0 for tungsten, with the lowest work function obtainable by cesium adsorption, was reduced to 0.62 Mv/cm.

Different enhancement factors are usually found for the two electrodes; this is illustrated by Fig. 6, which shows two Fowler-Nordheim plots of I-V data obtained by reversing the polarity of the electrodes. Since gap spacing (hence, gross field $F_0 = V/d$) and surface work functions were the same in both cases, the ratio of the slopes of the two curves is equal to the ratio of the maximum enhancement factors of the two electrodes.

Surface Geometry Changes Due to Temperature and Electric Field

The size and shape of protrusions on an electrode in vacuum, and thus the degree of surface roughness and the enhancement factor, can be changed by heating the electrode and by applying an electric field to its surface. For tungsten protrusions with sharp tips below approximately 1μ in radius and at temperatures below the melting point, it can be shown that the primary mechanism causing changes in radii is surface migration.[5,6] An expression for the change in protrusion length dz/dt due to surface migration has been derived and confirmed experimentally[6] for several refractory metals; it is approximately

$$\frac{dz}{dt} = -\frac{1.25\,S\Omega_0^2}{r^3 A_0}\frac{D_0 e^{-Q/kT}}{kT}\left(1 - \frac{rF^2}{8\pi S}\right) \qquad (1)$$

where Ω_0 and A_0 are the atomic volume and surface atom density, respectively, D_0 and Q are the diffusivity constant and activation energy for surface migration, S is the surface tension of the protrusion material, r the radius of the protrusion, T is temperature, and F the applied field.

In the absence of an electric field, the second term inside the brackets in Eq. (1) is zero, and the following expression can be derived for a protrusion having a terminal tip radius r and a conical shank with vertex half-angle α:

$$r^4 - r_0^4 = C\alpha t \qquad (2)$$

where r_0 is the initial tip radius of the protrusion, C is a function of temperature and properties of the protrusion material, and r is the radius obtained by heating at a temperature T for a time t. Because of the fourth power of the radius in Eq. (2), the variation of r with t is insensitive to the choice of α, and becomes insensitive to r_0 after sufficient heating such that $r \gg r_0$. Figure 7 shows Eq. (2) graphed in a form to give the approximate radius of a tungsten protrusion obtained when the surface is heated to a temperature T for various heating times, assuming a negligibly small initial tip

Table 1 Geometry changes due to heating

Electrode	γ	Emitting area, cm^2	Apex radius, cm
Sphere after arc	25.0	1.5×10^{-11}	2.2×10^{-6}
Sphere heated to 3000°K for 10 sec	11.0	2.2×10^{-9}	2.66×10^{-5}
Plane after arc	20.0	3.65×10^{-12}	1.08×10^{-6}
Plane heated to 1400°K for 180 sec	16.3	5.4×10^{-12}	1.3×10^{-6}

radius. It can be seen that, except by very prolonged heating at extremely high temperatures, it is difficult to obtain radii larger than a few microns by heating only. This means that a reduction in γ due to heating will occur if the tungsten protrusions have tip radii less than a micron, but that very little change will occur if the protrusions are large and have initial tip radii larger than a few microns.

The importance of the heating temperature on the magnitude of γ can be seen in Table 1, which presents data taken on both the sphere and the plane electrodes after an arc had occurred. Changes in γ and in effective emitting areas obtained from Eqs. (A1) and (A7), both before and after the arc, show that, generally, an arc roughened both anode and cathode, creating small protrusions. (Even though, in a few cases when γ was initially very large, an arc would, on the contrary, reduce γ). The results given in Table 1, obtained after heating two roughened surfaces to 1600° and 3000°K, respectively, verify the prediction of Eq. (2) and Fig. 7, namely, that heating to higher temperatures results in a smoother surface, i.e., in protrusions with γ lower and larger radii of curvature. In no case investigated, and despite favorable circumstances (i.e., the sphere was a single crystal, small diameter refractory metal electrode), was it possible to attain enhancement factors less than 10 by heating.

Application of an electric field affects surface migration of the substrate in two ways: 1) if the field is high enough and if the initial protrusion is large enough, it reverses the direction of migration so that the protrusions are enhanced, since the second term in the brackets of Eq. (1) will dominate; and 2) the field reduces the activation energy Q so that the migration rate increases.[7] We have some evidence of protrusion growth due to field-induced surface migration. In a field emission microscope, a positive field of 100 Mv/cm was applied to a smooth emitter heated at 1000°K; this produced a large number of protrusions in a short time with $\gamma \cong 3$ to 4 and an effective emitting area of $\sim 10^{-12}$ cm² (see Fig. 8). Also, when a negative field of 43 Mv/cm was applied to an emitter that already had a small protrusion on it, the protrusion was observed to grow even at room temperature. Thus, protrusions have been observed to grow under the influence of a high electric field of either polarity. The mechanism of nucleation of protrusions on a clean cathode surface by an electric field, as reported here, has not been positively identified; a possible mechanism would be nucleation by sputtering, which has been observed in the presence of high electric fields, on contaminated surfaces,[8] or even on clean surfaces in the presence of residual gas.[9]

It is interesting to note that our results suggest that protrusion growth, by field and temperature alone, is possible on both anode and cathode surfaces, in accordance with the observations of others[8]; however, the fields required for nucleation of the protrusions shown in Fig. 8 are higher than the maximum enhanced fields attained with gross electrode structures. It is possible that such mechanism for protrusion growth as field-induced surface migration or yield to field stresses may be more evident for lower melting metals or with differing surface conditions. In these cases, larger field enhancement factors and, hence, field emission currents at moderate gross field gradients might be expected.

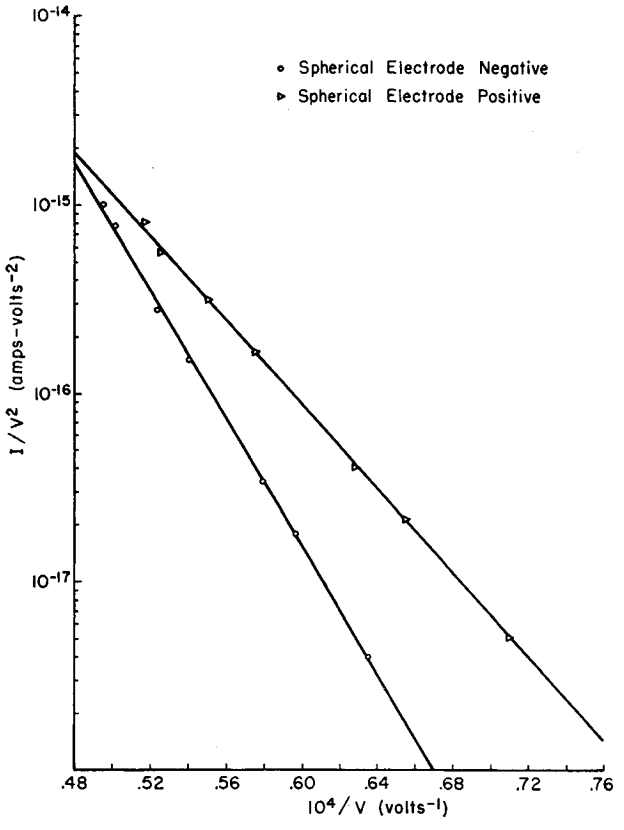

Fig. 6 Fowler-Nordheim plots of *I-V* data for both polarities of field at a constant gap spacing and work function.

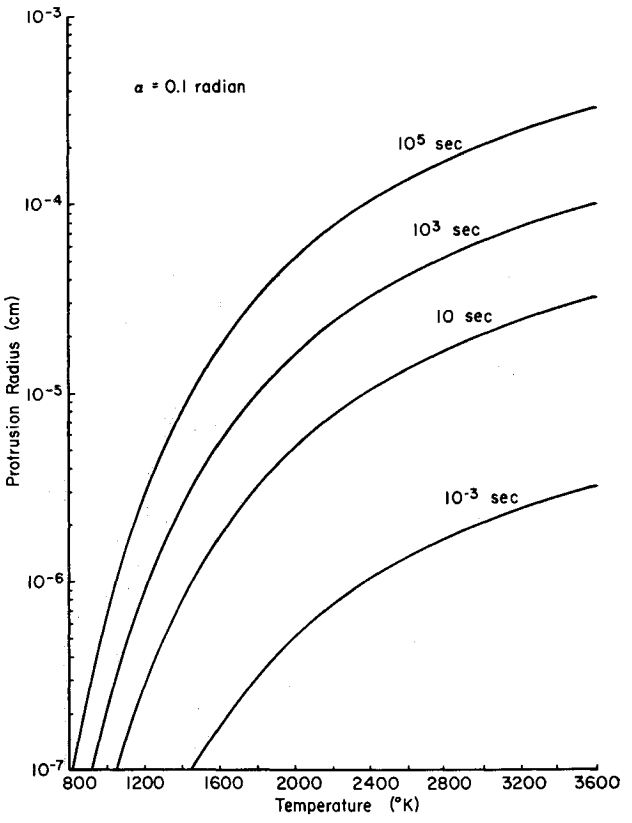

Fig. 7 Radius of a tungsten protrusion as a function of temperature for various heating times, for a conical protrusion with half-angle α = 0.1 rad and initial radius r_0 = 0.

Radiation Associated with Prebreakdown Current

Small pinpoints of light similar to those reported elsewhere in connection with electrical breakdown[8, 10–12] were observed on the anode when the current in the gap was 0.1 μa or larger. This radiation has been identified[13] as optical transition radiation, which occurs when a moving charged particle, in this case an electron, traverses a boundary between two media with different optical properties.[14, 15] There is no fundamental difference between transition radiation and Cerenkov radiation; for the former, the velocity of the charged particle is less than the speed of light in both media. Although transition radiation is not a factor contributing to the prebreakdown current, since it has been observed over several orders of magnitude range in current without causing deviations from field emission behavior, it does give some indication of how many protrusions are emitting. In some cases, particularly where the enhancement factor was quite low ($\gamma \cong 10$) only one spot of radiation was visible, whereas when the enhancement factor was large ($\gamma > 100$) several spots of radiation were observed, indicating that more than one protrusion on the surface was emitting. It can be shown[8] that, when more than one protrusion is emitting, the Fowler-Nordheim plots corresponding to the measured I-V characteristics will, in general, be linear, but the values of γ will be weighted strongly toward the highest values that could be calculated for each single emitter.

Effects of Cesium and Oxygen

Adsorption of cesium and/or oxygen on the electrode surfaces affects the prebreakdown gap current mainly through the changes caused in work function of the electrode surfaces. Figure 9 shows the variation in work function with cesium coverage for clean tungsten and for tungsten with two different underlying degrees of oxygen coverage. For cesium on clean tungsten the work function can vary as much as a factor of 3; the voltage across the gap would have to be reduced by about a factor of 5 in order to maintain a constant field-emitted gap current. For cesium on tungsten with a heavy coating of oxygen, the change in work function is very nearly a factor of 5; the corresponding reduction in gap voltage would be approximately a factor of 11 for a given field-emitted gap current.

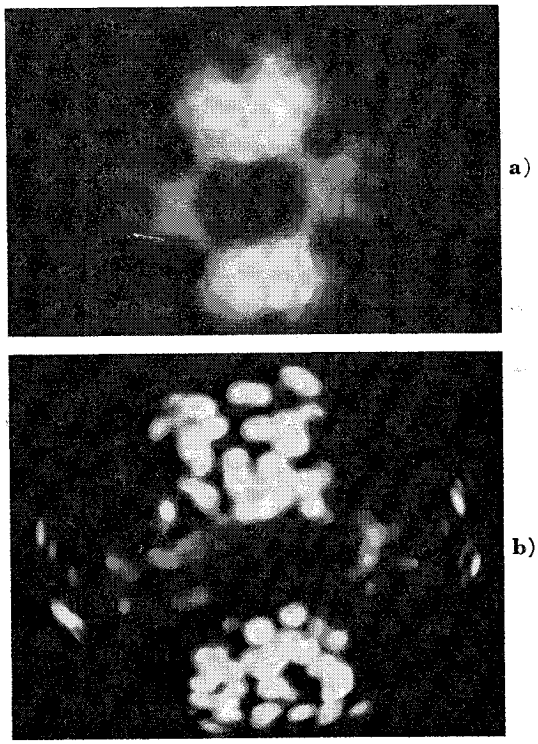

Fig. 8 Field emission patterns indicating the growth of protusions: a) initial pattern, I = 10 μa, V = 10kv; b) pattern after heating at 1600°K for 20 min with a positive field of 140 Mv/cm at the emitter surface, I = 10 μa, V = 3.4 kv.

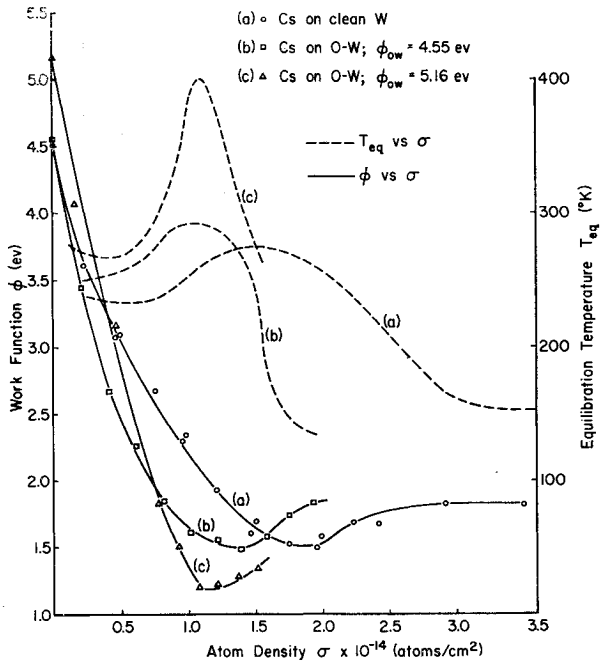

Fig. 9 Field emission work function (solid lines) and equilibration temperature (dotted lines) as functions of average cesium atom density for varying degrees of initial oxygen coverage.

The equilibration temperature curves of Fig. 9 are related to the mobility of cesium on the different substrates: the higher the equilibration temperature the less the mobility; they show that cesium is less mobile on oxygen-covered tungsten than on clean tungsten for a given degree of cesium coverage. The curves of Fig. 10 give the changes in work function due to thermal desorption of cesium from substrates with differing amounts of oxygen; they show that higher temperatures are required to desorb cesium from oxygen-covered tungsten than are necessary for cesium on clean tungsten. Thus, the general effect of oxygen is to bind the cesium more tightly to the surface, so that higher temperatures are required to change the work function of the surface.

The effect of increasing the cesium vapor pressure within the gap is to increase the cesium coverage on the electrodes for a given electrode temperature; for a cesium vapor pressure of 2×10^{-6} torr with electrodes at room temperature, the cesium coverage is greater than a monolayer. Our data indicate that, for the gap spacings (which are very much less than the mean free path of electrons within the cesium gas) and cesium pressure investigated, and for unheated electrodes, the prebreakdown gap currents are affected only through variations in work function. At higher cesium pressures, or at larger gap spacings, or at higher electrode temperatures, other mechanisms could become important. For example, at 300°K, desorption of cesium from the anode in ionic form can occur at fields of 20–50 Mv/cm, depending upon the coverage, by field desorption.[16] Under conditions reported here, no evidence of cesium ion formation by field desorption was observed, since the field at the anode was generally less than 20 Mv/cm when the electrodes were coated with cesium.

It has been reported elsewhere[17] that above 300°K an applied negative or positive field causes a corresponding reversible increase or decrease in the cesium coverage in the high field region due to a thermodynamically motivated diffusion process along the shank of the protrusion. At low

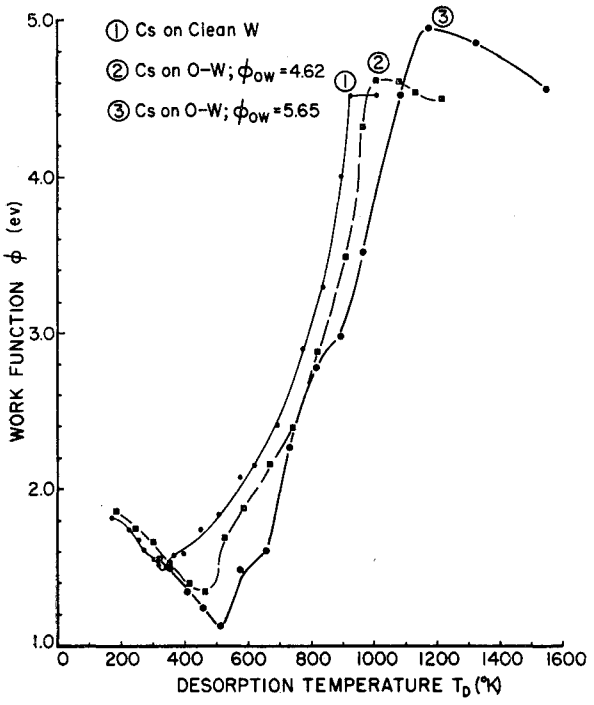

Fig. 10 Average field emission work function as a function of desorption temperature for cesium on the indicated substrates. The emitter was heated for 60 sec at the indicated temperature prior to each work function determination.

coverages (0.1 monolayer) and fields of 30 Mv/cm, the cesium coverage on the cathode is reduced by 50%. Such an effect has also been noted in this work and is illustrated in Fig. 11 where deviations from linearity of the Fowler-Nordheim plots are observed at high fields in the direction expected due to a reduction in cesium coverage. The shape of the curve after it deviates from linearity depends on the time between data points and the temperature of the surface. That the change in coverage is reversible can be deduced from the similarity in slopes (and hence, in associated work function) of curves 2 and the upper portion of curve 3 of Fig. 11, where the I-V data of curve 2 was obtained, and then the field was removed for a time sufficient to allow the cesium to return by surface diffusion to its initial coverage before data of curve 3 was taken.

It is interesting to note that for cesium coverages less than 0.7 monolayer the field-induced cesium coverage changes at the cathode increase the work function, i.e., decrease the field emission current, whereas the coverage changes at the anode result in a decrease of work function which reduces the rates of ion forming mechanisms, such as field desorption.[16] Thus, the field-induced cesium coverage changes at both electrodes are in the direction that opposes emission of charged particles into the gap, and hence in the direction that promotes gap stability and retards the onset of breakdown. The practical implication is that this effect tends to stabilize the prebreakdown current and increase the voltage that a given gap can withstand.

Concluding Remarks

Under the conditions investigated and reported here, i.e., very high vacuum, controlled amounts of contaminants on clean substrates, and controlled surface roughness, the prebreakdown gap current and gap voltage characteristic is stable, reproducible, and due to field emission. No evidence of ion generation or electrode sputtering was found, although under different conditions, such as higher gas pressures, larger gap spacings, and higher electrode temperatures, both of these may occur. The experiments reported in this paper have to do primarily with the origin and nature of gap currents detected prior to the onset of irreversible processes and electrical breakdown; however, the work is being extended into a more detailed study of the current-voltage characteristics up to the actual vacuum arc. Mechanisms by which field emission can lead into complete breakdown are discussed in detail elsewhere[8, 18–22]; in such cases, cesium coverage and enhancement factors should greatly alter the apparent breakdown fields. For clean electrodes or when the cathode has the higher enhancement factor, cathodic processes are likely to play a predominant role. Dyke et al.[21] have shown that high cathode current densities obtainable in field emission can resistively heat the cathode enough to vaporize some of the cathode material and cause an arc; they[18] have also derived the following expression relating the temperature at the tip of an emitter to its radius and the emitting current density J:

$$T_{\max} = 9.5 \times 10^{-4} J^2 r^2 \,^\circ\mathrm{C}$$

For $T_{\max} = 3000\,^\circ\mathrm{C}$, close to the melting point of tungsten, J varies between 2×10^9 and 2×10^7 amp/cm^2 for r between 10^{-6} and 10^{-4} cm. In the course of this investigation, electrical breakdown has been observed several times for clean tungsten electrodes; when observed, it occurred at field of 70 Mv/cm or higher and current densities exceeding 10^7 amp/cm^2 in accordance with the cathode resistive heating mechanism.

In addition, the experimental evidence generated here and elsewhere[22] indicates that, under certain conditions of field and temperature of the electrodes, changes in the geometry of protrusions can occur; these changes cause increases in γ, and thus, increases in field emitted gap current, which may in time culminate in a vacuum arc even though the gap voltage is held constant.

In conclusion, the work reported here establishes that: 1) for the conditions investigated, field emission is the dominant causes for prebreakdown (or leakage) current; 2) the occurrence of high local field enhancement factors, even on the most carefully treated electrode surfaces, indicates that in almost all cases electrode surfaces are subjected to local field considerably higher than the average potential gradient

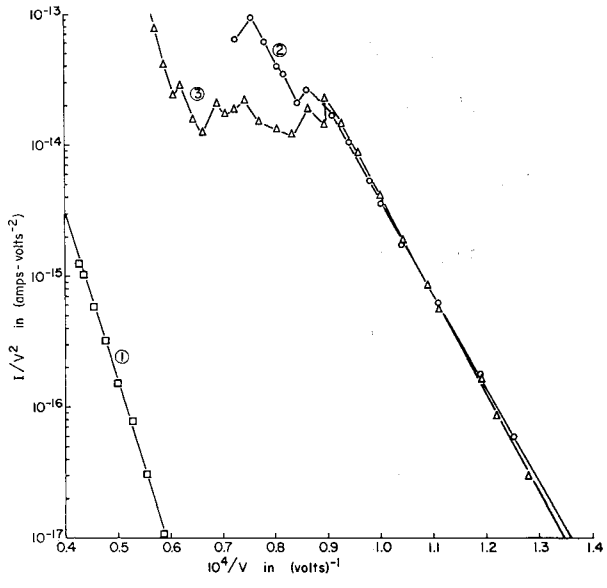

Fig. 11 Fowler-Nordheim plots obtained at room temperature with the sphere negative at a gap spacing of 4.5 mils. Curve 1 is for the clean tungsten surface. Curves 2 and 3 are for a cesium coverage corresponding to a work function of 2.9 ev. The deviation from linearity at high currents in curves 2 and 3 illustrates the field effect on the equilibrium cesium coverage as discussed in the text.

across the gap, making field emission a likely occurrence even though the gross fields are well below the values known to be required for field emission; 3) the presence of cesium affects the prebreakdown currents only through the changes it causes in surface work function; and 4) an applied electric field induces local changes in cesium coverage which inhibit the emission of charged particles across the gap.

Appendix

Since the field emission nature of the prebreakdown gap current was established, field emission techniques were used to analyze the data. These techniques are based on the experimentally confirmed Fowler-Nordheim law of field emission[23, 24] by analyzing the I-V data according to the following expression,[24] which contains the approximate correction for the Boltzmann tail to the Fermi distribution for a particular temperature range:

$$I(T, F) = P(T)AF^2 \exp(-b\phi^{3/2}/F) \quad \text{(A1)}$$

where A is directly proportional to emitting area and is a slowly varying function of ϕ, b is a constant, and

$$P(T, = \pi p/\sin\pi p \quad \text{(A2)}$$

in which p is given approximately by

$$p = kT2(2m_e)^{1/2}\phi^{1/2}/heF \quad \text{(A3)}$$

Substituting

$$F = \beta V \quad \text{(A4)}$$

(where β is a function of gap spacing and of geometry of an emitting protrusion only) into Eq. (A1) leads to an expression in terms of the directly measurable field emission current and voltage as

$$I = (BV^2) \exp(-2.3m10^4/V) \quad \text{(A5)}$$

It follows that a "Fowler-Nordheim plot" of the I-V characteristics (i.e., a plot of $\log_{10} I/V^2$ vs $10^4/V$) yields a straight line having a slope m and an intercept B with the vertical axis at $10^4/V = 0$. When the Fowler-Nordheim law is satisfied, it can be shown[24] that the work function ϕ is related to the slope m by the expression

$$m = -2.83 \times 10^3\phi^{3/2}/\beta \quad \text{(A6)}$$

In this work, the field F_0 for a smooth electrode surface is essentially V/d, since all gap spacings investigated (d from 1.5 to 10.0 mils) were smaller than the radius of the spherical electrode (12.5 mils). The local field F at the predominant field emission sources can be independently derived from the slope m of the Fowler-Nordheim plot and Eq. (A4); noting that $F = \gamma F_0$, and therefore $\beta = \gamma/d$, it is possible to determine γ in terms of the experimentally determinable parameters as follows:

$$\gamma = 2.83 \times 10^3\phi^{3/2}d/m \quad \text{(A7)}$$

Since γ is a function of electrode geometry only, it is, of course, independent of ϕ and d by virtue of Eq. (A6).

Using the work function ϕ_1 for the clean emitting surface as a reference, the work function ϕ_2 of the surface when coated with an adsorbate can be determined from

$$\phi_2 = \phi_1(m_2/m_1)^{2/3} \quad \text{(A8)}$$

where m_1 and m_2 are the slopes of the corresponding Fowler-Nordheim plots. When the average work function of the clean surface is well known, as in the case of clean tungsten ($\phi = 4.52$ ev), the work function of the coated surface can be determined with good accuracy. It should be emphasized that work functions so determined are automatically weighted toward the highly emitting (or low work function) planes of a poly crystal-face surface.

In summary, knowledge of ϕ, d, and the current and voltage for some particular point on the Fowler-Nordheim plot permits determination of γ, of the actual field at the emission site, as well as of the current density and the effective emitting area.[25] This information is all obtained from the I-V data without assuming any particular shape for the emitting protrusion or protrusions.

References

[1] Swanson, L. W., Strayer, R. W., and Charbonnier, F. M., "The variations of work-function with cesium coverage on molybdenum, tungsten and rhenium substrates," *Report on 24th Annual Conference on Physical Electronics*, edited by W. B. Nottingham (Technology Press, Cambridge, Mass., 1964), pp. 120–136.

[2] Dyke, W. P., Trolan, J. K., Dolan, W. W., and Barnes, G., "Field emitter: fabrication, electron microscopy, and electric field calculations," J. Appl. Phys. **24**, 570–576 (1953).

[3] Dyke, W. P. and Dolan, W. W., "Field emission," *Advances in Electronics and Electron Physics*, edited by L. Marton (Academic Press Inc., New York, 1956), Vol. 8, pp. 89–183.

[4] Gomer, R., *Field Emission and Field Ionization* (Harvard University Press, Cambridge, Mass., 1961).

[5] Boling, J. L. and Dolan, W. W., "Blunting of tungsten needles by surface diffusion," J. Appl. Phys. **29**, 556–559 (1957).

[6] Barbour, J. P., Charbonnier, F. M., Dolan, W. W., Dyke, W. P., Martin, E. E., and Trolan, J. K., "Determination of the surface tension and surface migration constants for tungsten," Phys. Rev. **117**, 1452–1459 (1960).

[7] Bettler, P. C. and Charbonnier, F. M., "Activation energy for the surface migration of tungsten in the presence of a high electric field," Phys. Rev. **119**, 85–93 (1960).

[8] Tomaschke, H. E., "A study of the projections on electrodes and their effect on electrical breakdown in vacuum," Coordinated Science Lab. Rept. R-192, Univ. of Illinois (January 1964).

[9] Martin, E. E., Trolan, J. K., and Dyke, W. P., "Stable high density field emission cold cathode," J. Appl. Phys. **31**, 782–789 (1960).

[10] Little, R. P. and Whitney, W. T., "Electron emission preceding electrical breakdown in vacuum," J. Appl. Phys. **34**, 2430–2432 (1963).

[11] DeGeeter, D. J., "Photographic observations of a prebreakdown discharge transition between metal electrodes in vacuum," J. Appl. Phys. **34**, 919–920 (1963).

[12] Mazeau, J. and Goldman, M., "Study of predischarges at very low pressures," Compt. Rend. **258**, 2774–2777 (1964).

[13] Bennette, C. J., Swanson, L. W., and Strayer, R. W., "Visible radiation from metal anodes preceding electrical breakdown," J. Appl. Phys. **35**, 3054–3055 (1964).

[14] Beck, G., "Contribution to the theory of the Cherenkov effect," Phys. Rev. **74**, 795–802 (1948).

[15] Frank, I. M., "Transition radiation and the Cerenkov effect," Soviet Phys.–Usp. **4**, 740–746 (1962).

[16] Utsugi, H. and Gomer, R., "Field desorption of cesium from tungsten," J. Chem. Phys. **37**, 1720–1722 (1962).

[17] Swanson, L. W., Strayer, R. W., and Charbonnier, F. M., "The effect of electric field on adsorbed layers of cesium on various refractory metals," Surface Sci. **2**, 177–187 (1964).

[18] Dolan, W. W., Dyke, W. P., and Trolan, J. K., "The filed emission initiated vacuum arc. II. The resistively heated emitter," Phys. Rev. **91**, 1054–1057 (1953).

[19] Alpert, D., Lee, D. A., Lyman, E. M., and Tomaschke, H. E., "Initiation of electrical breakdown in ultrahigh vacuum," J. Vacuum Sci. Tech. **1**, 35–50 (1964).

[20] Boyle, W. S., Kisliuk, P., and Germer, L. H., "Electrical breakdown in high vacuum," J. Appl. Phys. **26**, 720–725 (1955).

[21] Dyke, W. P., Trolan, J. K., Martin, E. E., and Barbour, J. P., "The field emission initiated vacuum arc. I. Experiments on arc initiation," Phys. Rev. **91**, 1043–1053 (1953).

[22] Brodie, I., "Studies of field emission and electrical breakdown between extended nickel surfaces in vacuum," J. Appl. Phys. **35**, 2324–2332 (1964).

[23] Fowler, R. H. and Nordheim, L. W., "Electron emission in intense electric fields," Proc. Roy. Soc. (London) **A119**, 173–181 (1928).

[24] Good, R., Jr. and Müller, E. W., "Field emission," *Handbuch der Physik*, edited by S. Flügge (Springer-Verlag, Berlin, 1956), Vol. 21, pp. 176–231.

[25] Charbonnier, F. M. and Martin, E. E., "A simple method for deriving, from measured $I(V)$ data, information on the geometry of a field emission current source of unknown characteristics," J. Appl. Phys. **33**, 1897–1898 (1962).